

Determining the ray propagator from traveltimes

D. Gajewski¹

keywords: ray propagator, paraxial rays, travel times

ABSTRACT

3-D prestack migration of the Kirchhoff type is still a task of enormous computational effort. Therefore, many implementations just compute traveltime tables and perform an unweighted summation stack along diffraction curves. At best some simplified migration weights are applied to obtain a “true amplitude” migrated image. However, to correctly determine reflection amplitudes, information on the wavefield dynamics in 3-D media like the ray propagator is essential. The ray propagator depends on the second derivative of traveltimes. It will be demonstrated in this paper, how these derivatives are determined from traveltimes without numerical differentiation. The ray propagator leads to important applications, since it provides an efficient technique to compute migration weights, dynamic (NMO) and divergence corrections, Fresnel zones or amplitudes. Another application of the ray propagator is the efficient and accurate interpolation of traveltimes, resulting in great savings of computational time and mass storage, since only coarse grid traveltime tables need to be computed and saved. The presented numerical examples indicate that the storage requirements of traveltime tables can be reduced by three orders of magnitude for 3-D data (i.e., instead of 30 GBytes of travel time tables you store only 30 MBytes). Since migration weights and the other above mentioned quantities can be computed “on the fly”, savings in mass storage are even considerably larger. It is sufficient to compute just coarse grid traveltime tables to perform a true amplitude prestack depth migration.

INTRODUCTION

Using Finite Difference (FD) eikonal solvers (Vidale, 1988, e.g.) or wave front construction (Vinje et al., 1993; Ettrich and Gajewski, 1996) traveltime tables are computed very efficiently. This is the foundation for the summation stack along diffraction surfaces for a Kirchhoff type migration. For a true amplitude migration, however, proper migration weights have to be applied in this summation (Schleicher et al., 1993a). The determination of the migration weights require the knowledge of wave-

¹email: gajewski@dkrz.de

field dynamics, like the wavefront curvature, i.e., second derivatives of the traveltimes. These derivatives build the foundation of the ray propagator, which can be used alternatively to determine migration weights, geometrical spreading, Fresnel zones or traveltime approximations (Hubral et al., 1992).

Numerical differentiation of traveltimes is a very unstable process and, therefore, not practical in real applications. Obtaining 2nd derivatives of traveltimes can be also achieved by dynamic ray tracing. This, however, is restricted to the ray tracing tools to generate traveltime tables and is involved with an increase in computational effort as well as an increase in mass storage requirements, since these derivatives have to be stored for later applications. Hubral et al. (1993) presented a procedure to compute the complete ray propagator from traveltime measurements. Their technique is based on the parabolic traveltime approximation. Two different experiments (zero-offset and CMP) are necessary to determine the propagator. Sun and Gajewski (1997) presented a procedure to compute migration weights from the kinematics of the wavefield, however, their technique is only applicable to the common source configuration.

In this paper we exploit the hyperbolic paraxial traveltime approximation to determine the complete propagator for any reflected ray in a arbitrary 3-D layered model from traveltime tables of shot gathers (which is usually the configuration used when traveltimes are computed). The knowledge of the propagator allows several applications important to exploration seismology, like divergence corrections, determination of migration weights for any source-receiver configuration as well as Fresnel zones and an efficient and accurate interpolation (up to the second order) of traveltimes.

METHOD

The technique to determine the 2nd derivatives of traveltime can be considered as an extension of the well known $T^2 - X^2$ method, however, for a 3-D model with heterogeneous layers, separated by curved interfaces. The 2nd derivatives of traveltimes are obtained by measuring slopes in $T^2 - X^2$ data fields. It corresponds to the local determination of linear moveout of squared traveltimes. The basic foundation for the procedure is given by the hyperbolic paraxial traveltime.

Hyperbolic paraxial traveltimes

We consider an arbitrary 3-D inhomogeneous layered medium with curved interfaces. A ray connecting the source S and the geophone G is considered, were the sources are located on a (curved) surface with coordinates s_I ($I=1,2$) and the geophones are located on a on surface with coordinates g_I ($I=1,2$). As mentioned above, we will not use the parabolic version of the paraxial traveltime as in Hubral et al. (1993), but its hyperbolic variant. This seems to be more appropriate, since it is known from the

investigation of layered media, that near vertical reflections are better approximated by hyperbolic rather than parabolic traveltimes curves (for a systematic investigation see also Ursin (1982)). The hyperbolic paraxial traveltimes reads (Schleicher et al., 1993b)

$$T^2(s_I, g_I) = [t_0 - p_I s_I + q_I g_I]^2 + t_0 [-2s_I N_{IJ} g_J + s_I \bar{N}_{IJ} s_J + g_I \tilde{N}_{IJ} g_J] \quad (1)$$

where t_0 is the traveltimes of the central ray (i.e. $s_I = 0$ and $g_I = 0$). p_I and q_I are slowness vectors of the central ray at the source and geophone, respectively, where two component notation is used (Bortfeld, 1989). The matrices N_{IJ} , \bar{N}_{IJ} and \tilde{N}_{IJ} represent second derivatives of traveltimes

$$N_{IJ} = \frac{\partial^2 t}{\partial s_I \partial g_J} \quad \bar{N}_{IJ} = \frac{\partial^2 t}{\partial s_I \partial s_J} \quad \tilde{N}_{IJ} = \frac{\partial^2 t}{\partial g_I \partial g_J} \quad ,$$

where the derivatives are taken at the central ray. From these derivatives the complete ray propagator can be constructed. These matrices are also the key ingredients for migration weights of any source-receiver combination, for Fresnel zones and for dynamic (NMO) and divergence corrections. The second derivatives also provide the foundation for the interpolation of traveltimes (accurate up to the second order). Eq. (1) is an approximation to the exact traveltimes, which is valid in a ‘‘paraxial vicinity’’ of the central ray. How large these vicinity might be, is investigated later in a numerical example for the interpolation of traveltimes.

Determining 2nd derivatives of traveltimes

Let us assume, we have computed traveltimes tables for a prestack-stack migration, i.e., traveltimes for many shots at every grid point of a discretized 3-D subsurface model are available. The determination of second derivatives of traveltimes reduces to measuring slopes similar to the well known $T^2 - X^2$ technique. To make this more obvious, we reduce the hyperbolic paraxial traveltimes equation into its 2-D form and for simplicity we assume that sources and receivers are located on straight lines. All matrices and vectors become scalars in this case, i.e.,

$$T^2(s, g) = [t_0 - ps + qg]^2 + t_0 [-2sNg + s^2\bar{N} + g^2\tilde{N}] \quad . \quad (2)$$

p and q correspond to the slowness projected onto the source and receiver line at the source and at the geophone, respectively, s and g are the offsets of the paraxial ray from the source and the geophone and $N = \partial^2 t / \partial s \partial g$, $\bar{N} = \partial^2 t / \partial s^2$, $\tilde{N} = \partial^2 t / \partial g^2$ are 2nd derivatives of traveltimes. If we further assume a laterally homogeneous layered model (i.e., $\bar{N} = -\tilde{N}$) and take a CMP gather, i.e., $s = -g$ with $s = r/2$ as half offset and considering the zero offset ray we arrive at the known result

$$T^2(r) = t_0^2 + \frac{1}{2} t_0 N r^2 = t_0^2 + \frac{r^2}{V_{NMO}^2}$$

where t_0 is the traveltime of the zero offset ray and V_{NMO} is moveout velocity (as a good approximation to the RMS-velocity of the Dix formula). From this equation it is obvious that the second derivative of traveltime is determined by the slope of the $T^2 - r^2$ graph or, in other words, by the linear moveout of squared traveltimes for the zero offset ray and the paraxial ray. The result also indicates, that N leads to a dynamic correction of the gather. The same conclusions apply to eqs. (1) and (2) but, please note, that these equations are valid for laterally heterogeneous media with curved interfaces and that they can be applied to any ray, not only the zero offset ray. The technique corresponds to locally fitting segments of hyperbolas to the real traveltime curve. In the following subsection we will describe the actual implementation of the procedure.

Implementation

We are not really interested in computing paraxial rays but we want to determine 2nd derivatives of traveltimes using properties of paraxial rays expressed through eq. (1) for the 3-D case or eq. (2) for the 2-D case. For simplicity we will explain the implementation for the 2-D situation but the extension to 3-D is straight forward. For prestack depth migration traveltime tables for many shots of a discretized subsurface model are computed. Fig.1 shows schematically such a traveltime grid where two shots are considered (S and S^x). Let us first fix the source position, (i.e., $s = 0$) and move the geophone (i.e., $g = dx$). Since we have directly computed the traveltimes $t(SG)$ at G and $t(SG^x)$ at G^x , we can solve for \tilde{N} in (2), i.e., $\tilde{N} = (t^2(SG^x) - [t(SG) + qdx]^2)/t(SG)dx^2$. All quantities on the right hand side are known. The traveltimes are taken from the tables, dx is given by the discretization of the subsurface. If ray tracing is used to generate the traveltime table also the slowness q is directly available. If FD eikonal solvers are used to generate the traveltimes, the gradient (slope) of the traveltimes determines the slowness approximately.

To determine \bar{N} we have to consider the traveltime $t(S^xG)$ at G of the neighboring shot S^x and again $t(SG)$ at G of shot S . The distance between S and S^x is $s = dx$, and the geophone position is fixed, i.e., $g = 0$. We solve (2) for \bar{N} , i.e., $\bar{N} = (t^2(S^xG) - [t(SG) - pdx]^2)/t(SG)dx^2$. To determine the remaining derivative N , we consider the traveltime $t(SG)$ of shot S at G and the traveltime $t(S^xG^x)$ of shot S^x at G^x . We solve again (2) for N where we use the results for \bar{N} and \tilde{N} obtained above. The above procedure is repeated for any grid point of the mesh except the boundaries. With the derivatives N , \bar{N} and \tilde{N} we can compute the geometrical spreading, migration weights or Fresnel zones, i.e., the ray propagator at any grid point of the discretized subsurface model (for details see, e.g., Hubral et al., 1992). Another application is the interpolation of traveltimes, which is demonstrated by a numerical example in the next section. Since eq. (1) is an approximation to the exact traveltime, the results are valid in a paraxial vicinity away from the central ray. How large this vicinity might be is

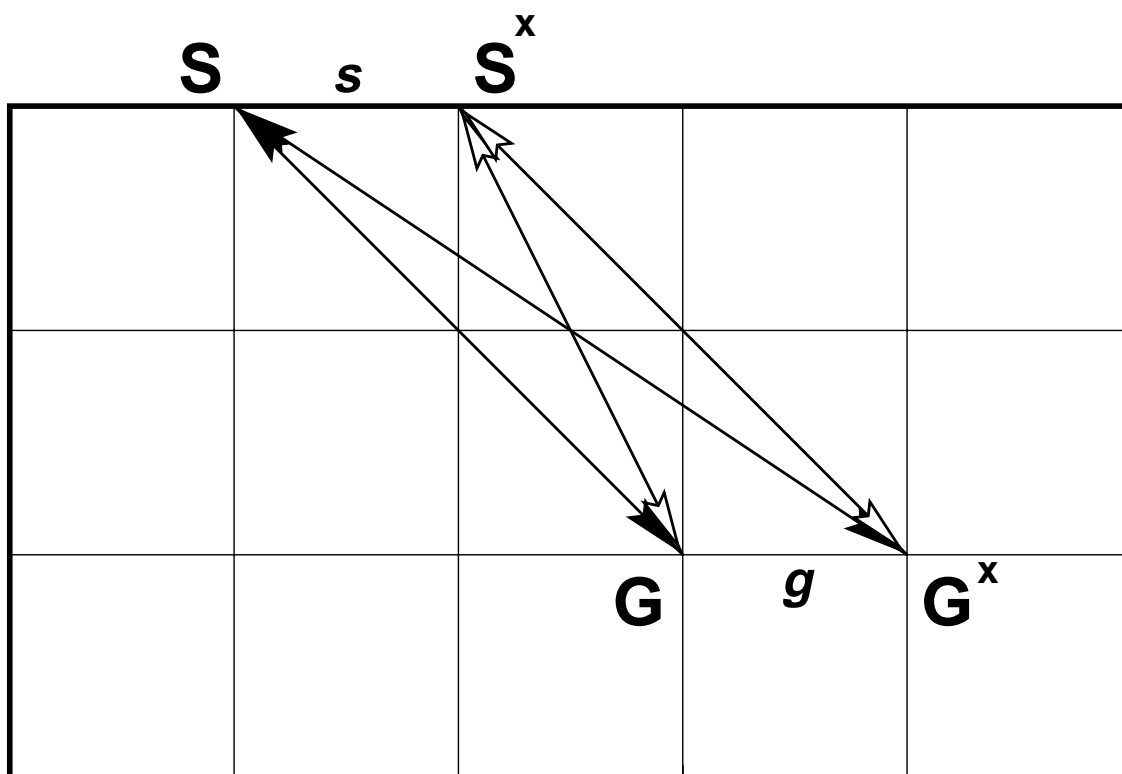


Figure 1: Traveltimes of source-geophone combinations for shots S and S^x to determine the complete ray propagator at G .

also discussed below.

APPLICATION: INTERPOLATION OF TRAVELTIMES

Eq. (1) and (2) can be used to interpolate traveltimes to any location between grid points. As it was described above, we can interpolate only horizontally. However, the same procedure to determine derivatives can be performed for vertical receiver lines. This allows to interpolate to any position between the grid points. In a first test a constant velocity model was investigated. Since both, diffraction and reflection curves are hyperbolic in this case, a good performance of eq. (2) to interpolate traveltimes is expected. Traveltimes computed on a coarse grid were interpolated onto a fine grid (number of samples was increased by a factor of 10 for each spatial direction) and compared with the exact results. The relative errors of exact and interpolated traveltimes were in the order of $10^{-5}\%$, i.e. in the order of machine accuracy for single precision word length. Although it is an expected result, since exact traveltime curves are hyperbolas it justifies the above described procedure.

The second numerical example of interpolating traveltimes is carried out for a model with a constant vertical gradient, i.e., $\partial v / \partial z = 0.5\text{s}^{-1}$ where the velocity at the surface is 3.0 km/s. Such a velocity model results in traveltime curves for diffractions and reflections which are non hyperbolic. The model dimensions are 2 km in horizontal direction and 1 km in vertical direction. A source at a distance and depth of 1 km is considered. The fine grid has 201x101 grid points and the coarse grid 21x11 grid point, i.e., in each spatial direction the number of grid points was reduced by a factor of 10. Traveltimes using a FD eikonal solver were computed to every grid point of the fine grid. This grid was resampled to the coarse grid size. 2nd derivatives of traveltimes for the coarse grid were computed according to the above described procedure. In the next step eq. (2) was used to interpolate traveltimes from the coarse grid onto the fine grid.

Fig. 2 shows the relative errors between the traveltimes computed directly on the fine grid and by interpolation from the coarse grid starting from a minimum distance of 100m from the source. The maximum relative error is below 0.2%. The error stays small (below 0.6%) even closer to the source where the wavefront curvature is strongest. For comparison, in Fig. 3, the relative errors obtained with the popular bilinear interpolation are shown (same gray scale, amplitudes greater than 0.2% are clipped). Here the maximum error is greater than 7%, and it increases even further for grid points more close to the source.

The performance of the hyperbolic paraxial interpolation using eq. (2) is considerably better, even far away from the source. Reducing the grid density by a factor of 10 in each spatial direction leads to tremendous savings in mass storage. However, the sampling interval of the coarse grid must match the velocity model such that the

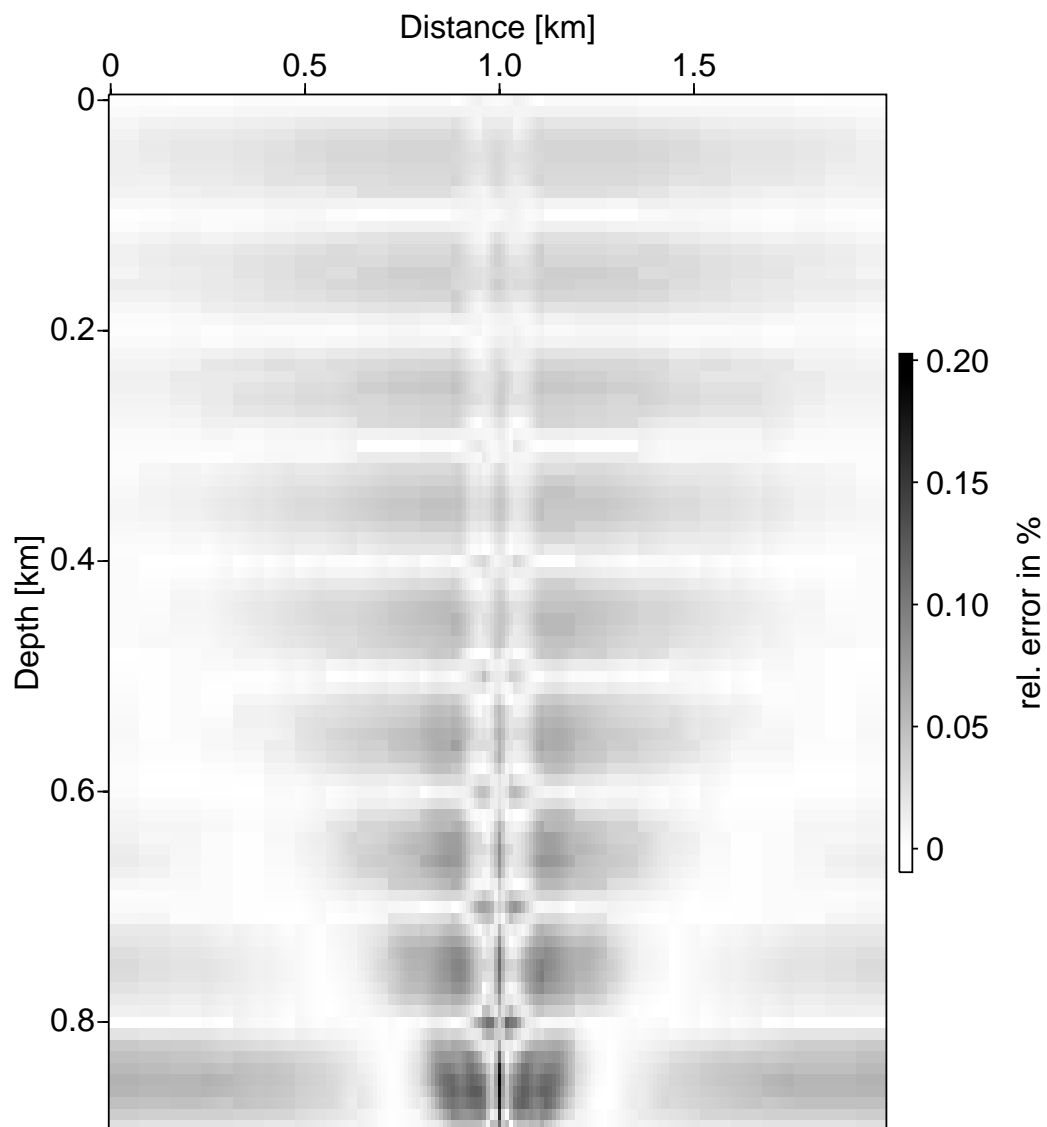


Figure 2: Relative errors between interpolated traveltimes computed from the coarse grid with the directly computed traveltimes of the fine grid. Maximum relative error is below 0.2%.

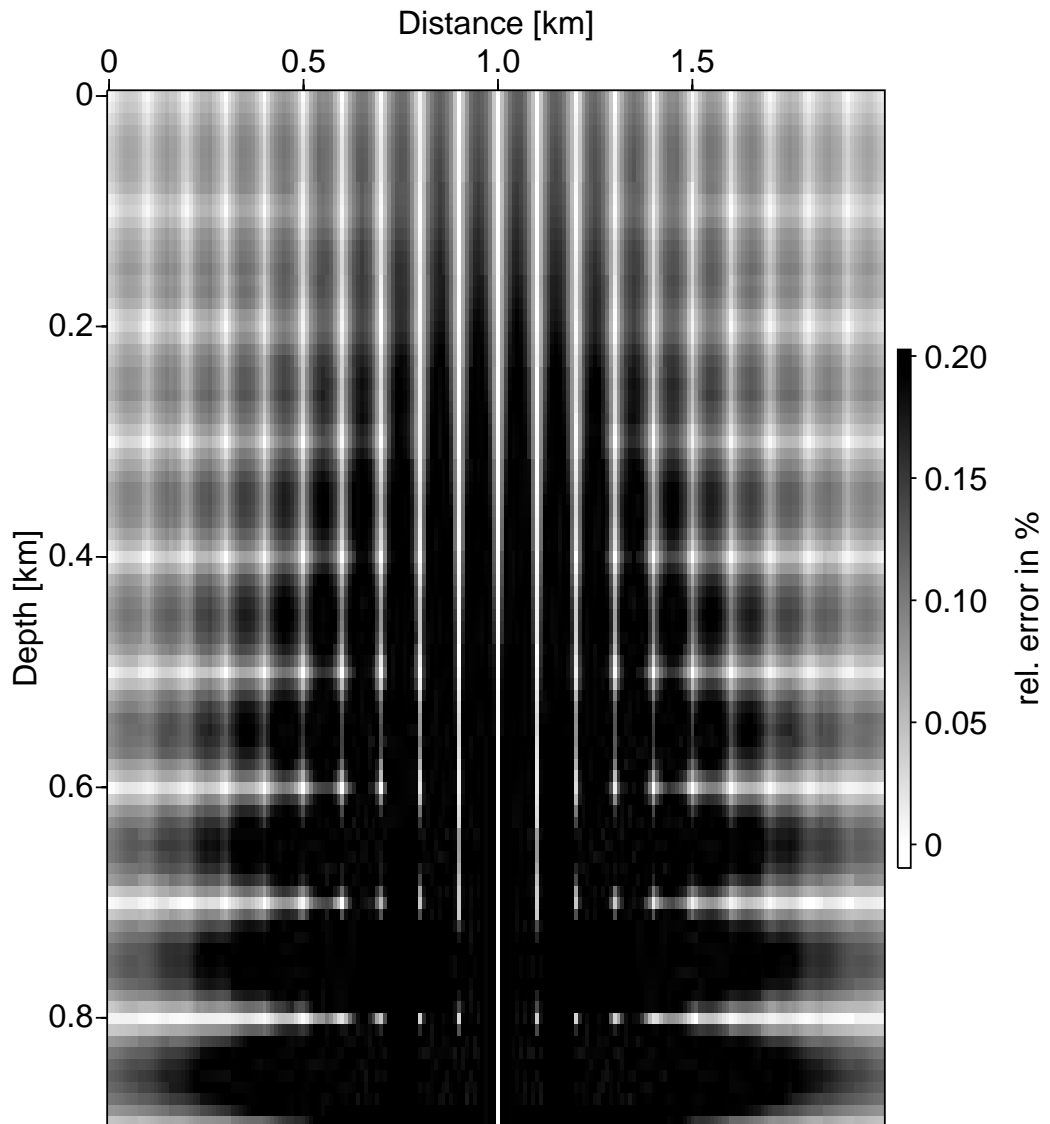


Figure 3: Relative errors between interpolated travel times computed from the coarse grid using bilinear interpolation with the directly computed travel times of the fine grid. Same grey scale as Fig. 2, amplitudes greater 0.2% are clipped. Maximum relative error is more than 7%.

smallest spatial variations of velocity are in the dimension of the coarse grid sampling. This may lead to a smaller grid steps of the coarse model. If the actual receiver sampling is, e.g., 20 m, a coarse grid model with a spatial sampling of 200 m might be too large. Please note, that eq. (1) or (2) do not require a uniform sampling for all spatial coordinates. The coarse grid might exhibit a faster sampling in the vertical direction, since velocity varies fastest with depth for most earth models. It is interesting to note that shots can be interpolated using eq. (1) or (2), i.e., traveltimes are computed only for a few shots, which are completed by interpolation.

CONCLUSIONS AND DISCUSSION

A procedure to determine the complete ray propagator from traveltimes was presented. The ray propagator has important applications in exploration seismology, like computation of migration weights, divergence corrections, and Fresnel zones. The ray propagator was used here for the interpolation of traveltimes from a coarse grid to a fine grid. It is quite common in prestack depth migration to generate traveltime maps on a coarse grid and to perform the actual migration on a fine grid which is obtained by interpolation. It was shown, that using an interpolation of traveltimes based on the hyperbolic paraxial traveltime is by far superior to the popular bilinear interpolation (and even paraxial approximation, not shown here), since the accuracy is higher. Using eqs. (1) or (2) not only traveltimes between receivers can be interpolated but also shot points. Since also the geometrical spreading can be derived from the ray propagator complete high-frequency Green's function can be computed.

In the numerical example the coarse grid was reduced in size by a factor of 10 for each spatial direction leading to tremendous savings in mass storage of the traveltime tables. Since all other quantities for migration like migration weights, divergence corrections or Fresnel zones are computed "on the fly" from the traveltime tables using the ray propagator, there is no need to save anything else than traveltime tables, leading to even higher savings in mass storage. We conclude, that it needs only coarse grid traveltime tables (and slownesses) to carry out a computationally efficient true amplitude aperture optimized (Fresnel zone based) migration using minimized mass storage. Introducing the eigenwave based traveltime expansion (Tygel et al., 1997), the number of operations to generate the ray propagator can be reduced resulting in an even faster procedure.

ACKNOWLEDGMENTS

This work was partially supported by the European Commission (JOF3-CT97-0029) and the sponsors of the WIT-consortium. Continuous discussions with the members of the Applied Geophysics Group are appreciated, particularly with Dr. Norman Ettrich,

Claudia Vanelle and Andree Leidenfrost. Norman also kindly provided a FD eikonal solver routine. I am grateful to Dan Kosloff, who initialized my interest in moveout based interpolation.

REFERENCES

- Bortfeld, R., 1989, Geometrical ray theory: Rays and traveltimes in seismic systems (second-order approximation of traveltimes): *Geophysics*, **54**, 342–340.
- Ettrich, N., and Gajewski, D., 1996, Wave front construction in smooth media for prestack depth migration: *PAGEOPH*, **148**, 481–502.
- Hubral, P., Schleicher, J., and Tygel, M., 1992, Three-dimensional paraxial ray properties, Part I: Basic relations: *J. Seis. Expl.*, **1**, 265–279.
- Hubral, P., Schleicher, J., and Tygel, M., 1993, Determination of fresnel zones from traveltme measuremnts: *Geophysics*, **58**, 703–712.
- Schleicher, J., Tygel, M., and Hubral, P., 1993a, 3-D true-amplitude finite-offset migration: *Geophysics*, **58**, 1112–1126.
- Schleicher, J., Tygel, M., and Hubral, P., 1993b, Parabolic and hyperpolic paraxial two-point travel times in 3D media: *Geophysical Prospecting*, **41**, 495–513.
- Sun, J., and Gajewski, D., 1997, True-amplitude common-shot migration revisited: *Geophysics*, **62**, 1250–1259.
- Tygel, M., Müller, T., Hubral, P., and Schleicher, J., 1997, Eigenwave based multi-parameter traveltme expansion: , *Soc. Expl. Geophys.*, 67th Ann. Internat. Mtg., 1770–1773.
- Ursin, B., 1982, Quadratic wavefront and traveltme approximations in inhomogeneous layered media with curved interfaces: *Geophysics*, **47**, 1012–1021.
- Vidale, J., 1988, Finite-difference calculation of traveltimes: *Bull. Seis. Soc. Am.*, **78**, 2062–2076.
- Vinje, V., Iversen, E., and Gjøystdal, H., 1993, Traveltme and amplitude estimation using wave front construction: *Geophysics*, **58**, 1157–1166.